

Neonatal Neuronal Circuitry Shows Hyperexcitable Disturbance in a Mouse Model of the Adult-Onset Neurodegenerative Disease Amyotrophic Lateral Sclerosis

Brigitte van Zundert,^{1,2} Marieke H. Peuscher,¹ Meri Hynynen,² Adam Chen,² Rachael L. Neve,³ Robert H. Brown Jr.,² Martha Constantine-Paton,¹ and Mark C. Bellingham^{1,4}

¹McGovern Institute for Brain Research, Massachusetts Institute of Technology, Cambridge, Massachusetts 02139, ²Day Laboratory for Neuromuscular Research, Department of Neurology, Massachusetts General Hospital, Charlestown, Massachusetts 02429, ³Department of Psychiatry, Harvard Medical School, McLean Hospital, Belmont, Massachusetts 02178, and ⁴School of Biomedical Sciences, University of Queensland, Brisbane, Queensland 4072, Australia

Distinguishing the primary from secondary effects and compensatory mechanisms is of crucial importance in understanding adult-onset neurodegenerative diseases such as amyotrophic lateral sclerosis (ALS). Transgenic mice that overexpress the G93A mutation of the human Cu-Zn superoxide dismutase 1 gene (hSOD1^{G93A} mice) are a commonly used animal model of ALS. Whole-cell patch-clamp recordings from neurons in acute slice preparations from neonatal wild-type and hSOD1^{G93A} mice were made to characterize functional changes in neuronal activity. Hypoglossal motoneurons (HMs) in postnatal day 4 (P4)–P10 hSOD1^{G93A} mice displayed hyperexcitability, increased persistent Na⁺ current (PC_{Na}), and enhanced frequency of spontaneous excitatory and inhibitory transmission, compared with wild-type mice. These functional changes in neuronal activity are the earliest yet reported for the hSOD1^{G93A} mouse, and are present 2–3 months before motoneuron degeneration and clinical symptoms appear in these mice. Changes in neuronal activity were not restricted to motoneurons: superior colliculus interneurons also displayed hyperexcitability and synaptic changes (P10–P12). Furthermore, *in vivo* viral-mediated GFP (green fluorescent protein) overexpression in hSOD1^{G93A} HMs revealed precocious dendritic remodeling, and behavioral assays revealed transient neonatal neuromotor deficits compared with controls. These findings underscore the widespread and early onset of abnormal neural activity in this mouse model of the adult neurodegenerative disease ALS, and suggest that suppression of PC_{Na} and hyperexcitability early in life might be one way to mitigate or prevent cell death in the adult CNS.

Key words: action potential; brainstem; dendrite; EPSP; IPSP; motor neuron; interneuron; locomotor activity; sodium channel; synaptic transmission; superior colliculus

Introduction

Amyotrophic lateral sclerosis (ALS) is a fatal paralytic disorder caused by adult degeneration of cranial and spinal motoneurons (Mulder, 1982). Average survival from symptom onset is 3–5 years, and treatment with riluzole only prolongs patient survival

by a few months (Cleveland and Rothstein, 2001). Approximately 25% of familial ALS (FALS) cases are caused by autosomal dominant mutations in the Cu-Zn superoxide dismutase 1 (SOD1) gene (Rosen et al., 1993). As in FALS patients, mice overexpressing the mutated human SOD1 (hSOD1) gene display progressive degeneration of motoneurons in adulthood (Gurney et al., 1994). However, the relationship between expression of the mutant gene and the proximal causes of motoneuron death in these intensively studied mouse lines remains obscure. Recent studies have provided important insights as to which cell types contribute to ALS pathology. Although mutant SOD1 causes intrinsic damage to motoneurons, non-neuronal cells may also contribute to the pathogenesis of motoneuron death (Clement et al., 2003; Boillée et al., 2006; Di Giorgio et al., 2007; Nagai et al., 2007). *In vitro* experiments show that conditioned media from cultured astrocytes expressing mutant hSOD1 can cause death of wild-type (WT) motoneurons (Nagai et al., 2007). However, it is still unclear how mutant hSOD1 in neuronal and non-neuronal cells causes motoneuronal pathology and death.

Studies with mutant hSOD1 transgenic mice *in vivo* and *in vitro* have identified many potentially pathogenic changes in mo-

Received March 28, 2008; revised Aug. 7, 2008; accepted Sept. 2, 2008.

This work was supported by National Institutes of Health Grant EY06039 (M.C.-P.); The Pierre L. de Bourgnecht ALS Research Foundation (B.v.Z., R.H.B.); the National Institute of Neurological Disorders and Stroke, the National Institute on Aging, the ALS Association, the Angel Fund, Project ALS, the Al-Athel ALS Foundation (R.H.B.), and the ALS Therapy Alliance (CVS Pharmacy) (R.H.B., M.C.B.); and The Motor Neuron Disease Research Institute of Australia and the National Health and Medical Research Council of Australia (M.C.B.). We thank A. J. Berger, J. Sebe, and R. Power for advice on hypoglossal motoneuron electrophysiological experiments and J. Durand for advice on the behavioral studies. B.v.Z. and M.C.B. performed all the electrophysiological experiments and analysis of electrophysiological data. M.H.P. performed all the HM structural analyses using HSV-GFP p1003, which was constructed and packaged by R.L.N. Behavioral testing was performed and analyzed by M.H. and A.C. B.v.Z., R.H.B., M.C.-P., and M.C.B. all contributed to the experimental design and the writing of this manuscript.

The authors declare no competing financial interests.

Correspondence should be addressed to Mark C. Bellingham, School of Biomedical Sciences, University of Queensland, Brisbane, Queensland 4072, Australia. E-mail: mark.bellingham@uq.edu.au.

B. van Zundert's present address: Department of Physiopathology, University of Concepción, Barrio Universitario s/n, Casilla C-160, Concepción, Chile.

DOI:10.1523/JNEUROSCI.1340-08.2008

Copyright © 2008 Society for Neuroscience 0270-6474/08/2810864-11\$15.00/0

toneurons, including excitotoxicity, disturbed Ca^{2+} homeostasis, mitochondrial dysfunction, SOD1 aggregation, cytoskeletal disruption, activation of cell death signals, and oxidative stress (Brown and Robberecht, 2001; Cleveland and Rothstein, 2001; Pasinelli and Brown, 2006). Nonetheless, the origin(s) and pathogenesis of motoneuron death in ALS remain largely unknown, because of the difficulty in distinguishing between primary target(s) of mutant SOD1 and secondary effects and compensatory mechanisms. This is particularly true for genetically induced diseases, in which effects of early expression of the aberrant gene can cause compensatory activity-dependent events in the developing CNS, masking overt symptoms until compensatory homeostasis breaks down as a result of subsequent trauma or aging (Clarke et al., 2001; DeKosky and Marek, 2003; Palop et al., 2006).

In $\text{hSOD1}^{\text{G93A}}$ mice, several pathogenic events in motoneurons, including mitochondrial dysfunction [as early as postnatal day 14 (P14)] and caspase-1 activation (P70), occur before clinical onset at 2–3 months and end-phase at 4.5 months (Gurney et al., 1994; Bendotti et al., 2001). To analyze functional changes in neuronal activity occurring during early development, we performed whole-cell patch-clamp recordings from hypoglossal motoneurons (HMs) in acutely prepared brainstem slices from P4–P10 $\text{hSOD1}^{\text{G93A}}$ mice. We found functional increases in persistent Na^+ current (PC_{Na}), hyperexcitability, and spontaneous synaptic transmission in these motoneurons. Similar functional changes were observed in neonatal superior colliculus (SC) interneurons (P10–P12), in which a precise timetable of synaptic development has been established in wild-type mice and in which we observed clearly precocial synaptic changes in $\text{hSOD1}^{\text{G93A}}$ mice. We also observed structural alterations in motoneuron dendritic architecture and locomotor behavior changes, consistent with precocial development and active compensatory adjustments for aberrant neuronal activity. The early onset of increased PC_{Na} and hyperexcitability in motoneurons suggests that these changes could contribute to later motoneuron death in the adult CNS.

Materials and Methods

Animals. All mice handlings were in accordance with the United States National Institute of Health guidelines and were approved by the Institutional Animal Care and Use Committees of Massachusetts Institute of Technology and Massachusetts General Hospital. In this study, hemizygous transgenic B6SJL mice carrying a high copy number of mutant human SOD1 ($\text{hSOD1}^{\text{G93A}}$) and WT human SOD1 (hSOD1^{WT}) were originally obtained from Jackson Laboratories. Nontransgenic littermates (mSOD1^{WT}) and hSOD1^{WT} mice were used as controls. Transgenic mice were identified by PCR as described earlier (Rosen et al., 1993). Genotyping was performed after the electrophysiological experiments had been performed to allow the experimenter to be “blind” to animal genotype. The $\text{hSOD1}^{\text{G93A}}$ mice, but not the mSOD1^{WT} or hSOD1^{WT} mice, develop initial signs of neuromuscular deficits (tremor of the legs and loss of extension reflex of the hindpaws) at ~10 weeks of age. At 18 weeks, they show marked locomotor impairment, with paralysis and muscular atrophy of the hind limbs. These animals die of respiratory failure at 20–21 weeks of age.

Slice preparations. Acute brainstem (P4–P10) and midbrain (P10–P12) slices were prepared as described previously (Bellingham and Berger, 1996; O’Brien and Berger, 1999; Aamodt et al., 2000; Shi et al., 2000; Townsend et al., 2003; Ireland et al., 2004). Animals were anesthetized with isoflurane and decapitated. The brainstem or the midbrain were quickly isolated and cut in 300- to 350- μm -thick transverse or parasagittal sections with a vibratome (Leica) in an ice-cold Ringer solution containing the following (in mM): 130 NaCl, 26 NaHCO_3 , 1.25 NaH_2PO_4 , 3 KCl, 10 glucose, 1 CaCl_2 , and 5 MgCl_2 , pH 7.35. Slices were

incubated at 35°C for 1 h in this Ringer solution and then maintained for at least another 0.5 h at room temperature (RT) in the same solution, except with 2 mM CaCl_2 and 2 mM MgCl_2 . Solutions were continuously bubbled with a 95% O_2 –5% CO_2 gas mixture.

Electrophysiology. Whole-cell recordings were made from HMs in brainstem slices (nXII) (Bellingham and Berger, 1996; O’Brien and Berger, 1999; Ireland et al., 2004) and SC interneurons in the stratum griseum superficiale of superior colliculus slices (Aamodt et al., 2000; Shi et al., 2000; Townsend et al., 2003). Recording artificial CSF (ACSF) contained the following (in mM): 130 NaCl, 26 NaHCO_3 , 1.25 NaH_2PO_4 , 3 KCl, 10 glucose, 2 CaCl_2 , and 1–4 MgCl_2 , bubbled with 95% O_2 /5% CO_2 , pH 7.35. For recording action potential (AP) firing and voltage-dependent currents, a K gluconate-based internal solution was used, containing the following (in mM): 17.5 KCl, 122.5 K gluconate, 9 NaCl, 1 MgCl_2 , 10 HEPES, 0.2 EGTA, 3 MgATP , and 0.3 GTP-Tris. For recording synaptic currents, a Cs gluconate-based internal solution was used, containing the following (in mM): 122.5 Cs gluconate, 17.5 CsCl, 8 NaCl, 10 HEPES, 0.2 EGTA, 2 MgATP , and 0.3 GTP-Na. After formation of a high-resistance seal ($>1\text{G}\Omega$) and break-in, only neurons with series resistance $<40\text{M}\Omega$ and input resistance of $>500\text{M}\Omega$ (SC interneurons) or $>50\text{M}\Omega$ (HMs) were used for subsequent analysis. Whole-cell voltage or current signals were recorded with an Axopatch 200B amplifier (Molecular Devices). Pipette and whole-cell capacitance and series resistance were compensated using amplifier circuitry. Signals were low pass filtered (1–10 kHz) and digitized (5–40 kHz) on a PC using pClamp software, and measured and analyzed with Clampfit 8.0–10, MiniAnalysis (Synsoft), Excel (Microsoft), and Prism 4 (Graphpad).

Recording of AP firing and voltage-dependent currents were performed with complete blockage of ionotropic synaptic transmission by addition of a mixture of antagonists against AMPA receptors (AMPA) (10 μM DNQX), NMDA receptors (NMDARs) (50 μM D-APV), glycine receptors (GlyRs) (2 μM strychnine HCl), and GABA_A receptors (GABA_ARs) [5 μM bicuculline methiodide (BMI)]. To record synaptic currents mediated by only NMDARs, AMPARs, GABA_ARs, or GABA_AR/GlyR, different mixtures of these antagonists were applied to the bath solution, as previously used for SCs (Aamodt et al., 2000; Shi et al., 2000; Townsend et al., 2003) and for HMs (Bellingham and Berger, 1996; O’Brien and Berger, 1999). Thus, spontaneous AMPAR-mediated EPSCs were isolated by the addition of D-APV, strychnine, and bicuculline. The remaining synaptic currents were AMPAR mediated, because they were completely abolished after recordings by bath application of DNQX. In some experiments, quantal AMPAR-mediated currents were isolated by additional bath application of the sodium channel blocker TTX (0.5–1 μM) with or without bath application of CdCl_2 (100 μM). Spontaneous NMDAR-mediated EPSCs were isolated in Mg^{2+} -free ACSF by the addition of DNQX, strychnine, and BMI. The remaining synaptic currents were NMDAR mediated, because they were completely abolished subsequently by addition of D-APV to the ACSF. Spontaneous GABA_AR/GlyR-mediated IPSCs were isolated by the addition of D-APV and CNQX. In SC interneurons, these IPSCs were mediated only by GABA_ARs, because they were completely abolished by subsequent bath application of BMI (Aamodt et al., 2000; Shi et al., 2000). In HMs, the IPSCs were mediated by a mixture of GlyRs and GABA_ARs, because addition of both strychnine and BMI were required to completely abolish them (Bellingham and Berger, 1996; O’Brien and Berger, 1999). For all synaptic current recordings, neurons were held at a membrane potential of -70mV , except for recordings of GABA_AR mediated activity in SC interneurons, which were recorded at $+50\text{mV}$ for comparison to previous SC interneuron data (Aamodt et al., 2000; Shi et al., 2000).

Spontaneous events were detected and measured over a total of 75 s of continuous recording, chosen randomly throughout the recording period for each neuron. Baseline noise ranged from 2.5 to 5.0 pA peak to peak, and synaptic events with an amplitude >2 times 1/2 peak-to-peak noise were analyzed. Synaptic currents were characterized by the following parameters: peak amplitude, interval between sequential currents, rise time (from 10 to 90% of peak amplitude), and decay time. Decay time was determined by fitting the synaptic current decay from 100 to 0% peak amplitude with a single exponential and is given in milliseconds throughout the text as decay interval measured at 0.37 peak amplitude of

the fitted exponential. The mean for each parameter for all synaptic events recorded from individual neurons was obtained using MiniAnalysis 5.1 and Prism 4.

HM labeling. Construction and packaging of HSV amplicon vector p1003 containing the green fluorescent protein (GFP) driven by a CMV promoter has been described previously (Neve et al., 2005; Olson et al., 2005). To retrogradely label HMs in the ipsilateral hypoglossal nucleus (nXII), P1 animals were deeply anesthetized by hypothermia and 1–2 μ l of HSV-GFP p1003 (2×10^8 /ml) was slowly pressure-injected into the tip of the tongue muscle with a borosilicate glass electrode pipette ($>50 \mu$ m tip diameter) held in a micromanipulator. The mice were monitored until they recovered spontaneous movement and allowed to survive till P6 before being killed. For immunohistochemistry, mice were deeply anesthetized with pentobarbital, and intracardially perfused with 4% paraformaldehyde and 0.5% glutaraldehyde. Brains were removed, post-fixed overnight in the same fixative, and maintained in a 30% sucrose-PBS solution for >12 h at 4°C before being processed further. To analyze the infected HMs, 250 μ m sequential vibratome sections through the entire brainstem were cut, and sections were permeabilized in 0.5% Triton X-100/PBS for 2 h at RT and then blocked with 10% normal horse serum for 2 h at RT. Sections were then incubated with a rabbit anti-GFP antibody coupled to Alexa-488 (Invitrogen) overnight at 4°C in 0.025% Triton X-100/PBS. After washing and mounting, the sections were analyzed using a Nikon PCM 2000 confocal microscope equipped with an argon laser and appropriate performance filters for detection of GFP.

Behavioral testing. Six sensorimotor responses appearing from P1 to P12 were measured daily in all male and female mice as described previously (Amendola et al., 2004). When the appropriate responses were observed, the pup was given a score of 1 for the corresponding test. The following tests were performed: (1) righting: the pup was placed on its back and was tested to right itself within 10 s. (2) Cliff-drop aversion: the pup was placed on the edge of a cliff (with its forepaws and the head over the edge) and was tested to turn and crawl away from the cliff. (3) Forepaw and (4) hindpaw grasping: the inside of one paw of the pup was gently stroked with an object, and the ability to flex the paw and grasp the object was tested. (5) Forelimb placing: the dorsum of one paw was touched with the edge of an object, and the ability to lift the paw and place it on the object was tested. (6) Vibrissae placing: the pup was suspended by the tail and was tested to raise its head and carry out a placing response with the extended forelimb when the vibrissae touched a pencil.

Data analysis. Data are expressed as arithmetic mean \pm SE. Statistically significant differences were determined using Student's unpaired *t* test (electrophysiology and structural changes) or χ^2 test (animal behavioral studies) except where noted. For all statistical tests, values of $*p \leq 0.05$, $**p \leq 0.01$, and $***p \leq 0.001$ were considered statistically significant.

Results

Hyperexcitability in presymptomatic hSOD1^{G93A} motoneurons and interneurons

As in FALS patients, hSOD1^{G93A} mice display a progressive degeneration of motoneurons in adulthood (beginning at 2.5–3 months after birth) (Gurney et al., 1994). This restricted cell death of adult motoneurons cannot be explained by the spatio-temporal expression of mutant SOD1, because hSOD1^{G93A} in FALS patients and in transgenic mice is expressed ubiquitously in all cells of the CNS throughout life (Gurney et al., 1994). To analyze whether normal brain function is disturbed during early development, we performed whole-cell patch-clamp recordings from HMs in acutely prepared brainstem slices from P4–P10 hSOD1^{G93A} and mSOD1^{WT} mice. We first analyzed whether HMs in brain slices display increased intrinsic excitability at this early stage of development, as occurs in dissociated cultured spinal cord neurons derived from embryonic hSOD1^{G93A} mice (Kuo et al., 2004). To analyze intrinsic excitability, we recorded AP firing in response to depolarizing current steps (Fig. 1A). We found that hSOD1^{G93A} HMs fired at significantly higher rates than HMs in brainstem slices from mSOD1^{WT} mice (Fig. 1A,B);

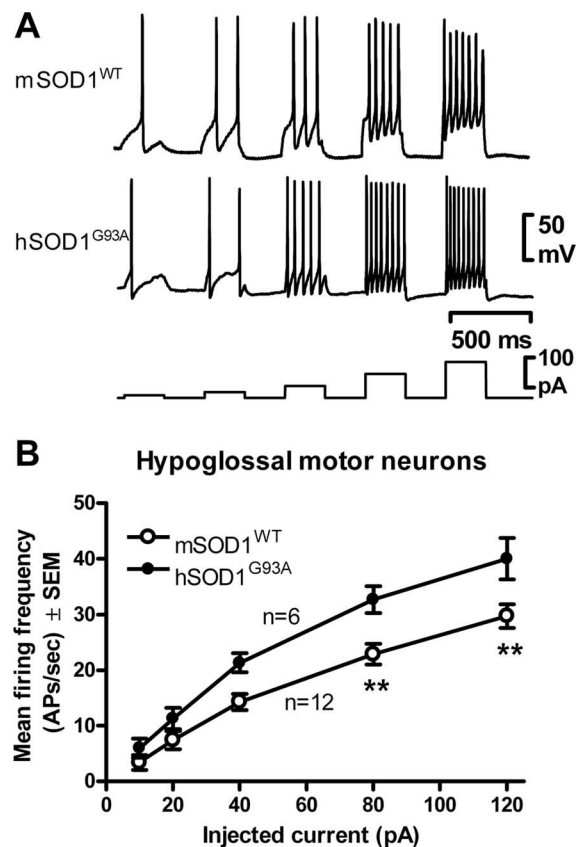


Figure 1. Intrinsic excitability is increased in HMs from presymptomatic hSOD1^{G93A} ALS mice. HMs in acutely prepared brainstem slices of mSOD1^{WT} and hSOD1^{G93A} mice were recorded. **A**, Membrane potential sample traces in mSOD1^{WT} (top) and hSOD1^{G93A} HMs (middle) showing APs evoked by rectangular depolarizing current pulses (bottom; 10–120 pA, 300 ms, 0.5 Hz). **B**, Mean AP frequency plotted against injected current show that the intrinsic excitability in hSOD1^{G93A} HMs ($n = 6$) is significantly increased compared with mSOD1^{WT} HMs ($n = 12$). Statistical significance is indicated.

mean firing rates with current injections of 80 and 120 pA were 22.9 ± 1.9 and 29.7 ± 2.1 Hz in 12 mSOD1^{WT} HMs, and 32.7 ± 2.4 and 40.0 ± 3.7 Hz in 6 hSOD1^{G93A} HMs (repeated-measures ANOVA, Bonferroni posttest). In addition, we also analyzed firing rates of HMs from hSOD1^{WT} mice. We found that the firing rates of two hSOD1^{WT} HMs (24.0 ± 4.0 and 28 ± 4 Hz at 80 and 120 pA; data not shown) were similar to mSOD1^{WT} HMs and significantly lower than those of hSOD1^{G93A} HMs (repeated-measures ANOVA, Bonferroni posttest). This finding supports the idea that motoneuron hyperexcitability was specifically attributable to the hSOD1^{G93A} mutation and not to effects of overexpression of the hSOD1 protein. Thus, HMs in acutely prepared brainstem slices from early postnatal hSOD1^{G93A}-overexpressing mice show intrinsic hyperexcitability, 2–3 months before cell death and clinical symptoms appear.

To investigate the basis for this hyperexcitability, we analyzed several cell properties and AP characteristics of mSOD1^{WT} and hSOD1^{G93A} HMs. Although no differences in AP firing threshold, AP duration, afterhyperpolarization amplitude, resting membrane potential, or input resistance were found between mSOD1^{WT} and hSOD1^{G93A} HMs, the AP amplitude of hSOD1^{G93A} HMs was significantly increased compared with mSOD1^{WT} motoneurons (Table 1). As inhibition of 60% of available Na⁺ channels reduces AP amplitude by 10 mV in other central neurons (Raman and Bean, 1999), our observation of a 20

Table 1. Hypoglossal motoneuron properties

	mSOD1 ^{WT}	hSOD1 ^{G93A}
Cell properties		
Resting membrane potential (mV)	−59 ± 5	−61 ± 6
Input resistance (MΩ)	111 ± 18	106 ± 18
Action potential properties		
Threshold (mV above resting MP)	21 ± 3	22 ± 3
Amplitude (mV above threshold MP)	69 ± 4	87 ± 4*
Maximum rate of AP rise (mV/ms)	189 ± 32	232 ± 56
Duration (ms)	3.7 ± 0.5	3.0 ± 0.4
Half-width duration (ms)	1.6 ± 0.2	1.4 ± 0.2
Afterhyperpolarization amplitude (mV below threshold MP)	−27 ± 2	−29 ± 3
Number of cells	7	7

Averaged cell properties and AP properties (analyzed from single APs) are shown for mSOD1^{WT} and hSOD1^{G93A} HMs (P6–P8). In this table and Table 2, resting membrane potential has been corrected for a calculated junction potential of 13 mV (JPCalc, Clampfit). AP threshold is relative to resting membrane for each HM recorded; AP and afterhyperpolarization amplitude are relative to AP threshold potential for each HM recorded. Note that only the AP amplitude is significantly increased in hSOD1^{G93A} HMs. Statistical significance (Student's unpaired *t* test) is indicated. Data are mean ± SEM.

mV increase in AP amplitude suggested that increased Na⁺ channel density may contribute to hyperexcitability in developing hSOD1^{G93A} HMs. Accordingly, we measured the maximum rate of rise of individual APs, because this measurement is more directly related to Na⁺ channel density than AP amplitude (Kole et al., 2008); however, mean maximal rate of AP rise was not significantly increased in HMs from hSOD1^{G93A} mice (Table 1).

Recently, it has been shown that cultured spinal cord neurons derived from embryonic hSOD1^{G93A} mice displayed an increased PC_{Na}, capable of amplifying a neuron's response to excitatory synaptic inputs and enhancing its repetitive firing capability with prolonged depolarization (Kuo et al., 2005). To test whether a PC_{Na} is present in early postnatal HMs and contributes to regulation of HM repetitive firing, we bath applied riluzole (20 μM). Riluzole inhibits PC_{Na} but has relatively small inhibitory effects on the fast inactivating Na⁺ current, which generates APs (Urban and Belluzzi, 2000). Riluzole did not prevent AP generation at the current step onset but significantly reduced repetitive AP firing in response to current injection in mSOD1^{WT} HMs (Fig. 2A), demonstrating that PC_{Na} was present in neonatal HMs.

Next, we directly recorded isolated PC_{Na} to determine whether PC_{Na} is increased in hSOD1^{G93A} HMs. Voltage-dependent inward currents were evoked by slow voltage ramps from −60 mV to +10 mV and back (8 s total duration) (Fig. 2B5) with bath-applied CdCl₂ (100 μM) to block voltage-gated Ca²⁺ channels (Carlin et al., 2000; Powers and Binder, 2003). In both mSOD1^{WT} and hSOD1^{G93A} HMs, an inward current was progressively activated at voltages above −60 mV, with peak current at −30 to −10 mV (Fig. 2B1–B4, gray line). This inward current was a PC_{Na}, because it was abolished by either riluzole (20 μM) (Fig. 2B1,B3, black line) or 500 nM TTX (Fig. 2B2,B4, black line), a highly specific Na⁺ channel antagonist that blocks both PC_{Na} and AP generation (Goldin, 1999). After normalizing whole-cell current for cell membrane area (determined by measurement of whole-cell capacitance), the mean peak amplitude of the PC_{Na} current–voltage relationship for individual HMs from hSOD1^{G93A} mice (mean of 16.6 ± 3.3 pA/pF, *n* = 12) was significantly increased (*p* < 0.05, unpaired *t* test), approximately threefold compared with the mean PC_{Na} peak amplitude in HMs from mSOD1^{WT} mice (mean of 6.0 ± 2.2 pA/pF, *n* = 9), without alterations in the voltage dependence of PC_{Na} (Fig. 2C). Together, these results strongly suggest that increased PC_{Na} is a key mechanism causing intrinsic hyperexcitability in early postnatal HMs from hSOD1^{G93A} mice.

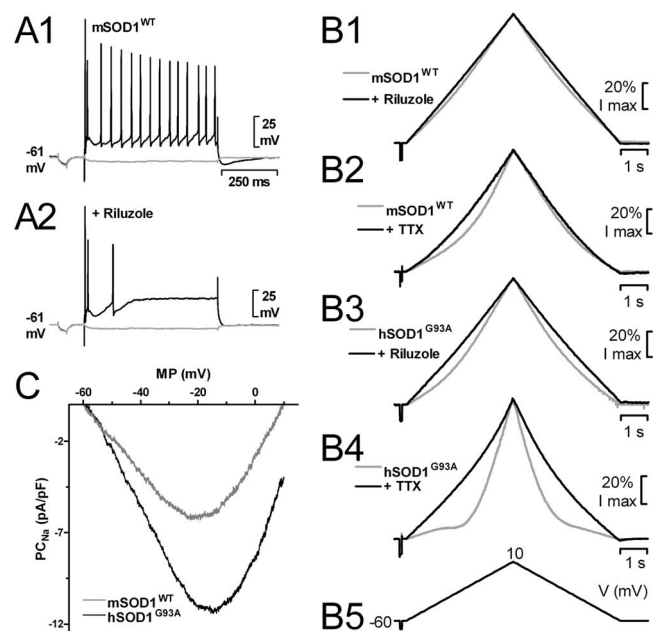


Figure 2. PC_{Na} is increased in HMs from presymptomatic hSOD1^{G93A} ALS mice. **A**, AP sample traces in a mSOD1^{WT} HM without (**A1**) and with (**A2**) riluzole (20 μM). Note that riluzole is unable to prevent AP generation at the current step onset but abolishes repetitive AP firing without changing subthreshold responses (gray traces). **B**, PC_{Na} current traces generated by a slow (total 8 s) triangular voltage-clamp command (**B5**) from a holding potential of −60 to 10 mV and recorded from mSOD1^{WT} HMs in the absence (gray traces) and presence of riluzole (20 μM, black traces; **B1**) or TTX (500 nM, black traces; **B2**) or from hSOD1^{G93A} HMs (riluzole, **B3**; TTX, **B4**). Note that PC_{Na} (which is the TTX-sensitive inward current activated at voltages more than −40 mV) is significantly larger in the hSOD1^{G93A} HM. **C**, Current–voltage relationship of mean PC_{Na} current normalized to cell capacitance (current density) plotted against voltage ramp membrane potential (MP) for mSOD1^{WT} HMs (*n* = 9) and hSOD1^{G93A} HMs (*n* = 12), showing that the voltage dependence of PC_{Na} is unchanged in hSOD1^{G93A} HMs.

We reasoned that if generation and repetitive firing of APs is an essential feature of most neurons and expression of mutant SOD1 is ubiquitous in CNS neurons, intrinsic hyperexcitability might not be unique to motoneurons in hSOD1^{G93A} mice. Hyperexcitability might therefore also occur in interneurons, such as in SC interneurons that control eye movements, a function that remains relatively normal in human ALS patients until the final stages (Kaminski et al., 2002). In addition, SC interneurons undergo well characterized and precisely timed developmental changes in synaptic transmission. At the end of the second postnatal week (P13–P14), when visual activity increases with retinal maturation and eye-opening, frequency of spontaneous synaptic activity mediated by AMPARs (sAMPA) and GABA_ARs (sGABA) increases, whereas NMDAR currents (sNMDAs) decay faster because of a change in the composition from NR2B-rich to NR2A-rich receptors (Shi et al., 1997, 2000; Aamodt et al., 2000; Colonnese et al., 2003; Lu and Constantine-Paton, 2004; Townsend et al., 2004; van Zundert et al., 2004). The dependence of these synaptic changes on neural activity led us to predict that hyperactivity would be associated with accelerated development of synaptic transmission in hSOD1^{G93A} mice.

We first examined the excitability of SC interneurons. As predicted, hSOD1^{G93A} SC interneurons in acutely prepared mid-brain slices from hSOD1^{G93A} P10–P12 mice also fired at higher frequencies (30.9 ± 4.3 Hz at 120 pA, *n* = 7) than SC interneurons from mSOD1^{WT} mice of the same age group (18.5 ± 4.1 Hz at 120 pA, *n* = 8; *p* < 0.05, repeated-measures ANOVA, Bonferroni posttest) (Fig. 3A,B). Apart from a significant increase in AP

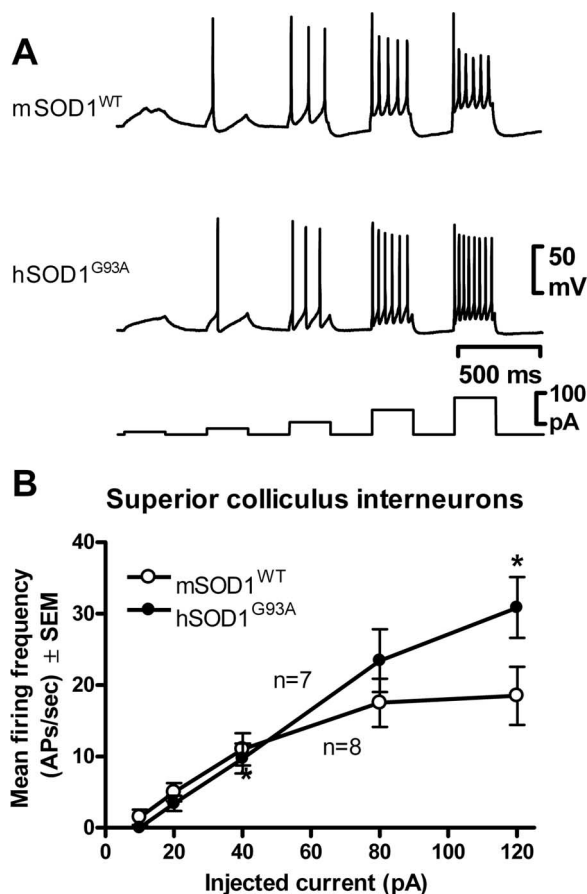


Figure 3. Intrinsic excitability is increased in SC interneurons from presymptomatic hSOD1^{G93A} ALS mice. SC interneurons of acutely prepared midbrain slices of mSOD1^{WT} and hSOD1^{G93A} mice were recorded. **A**, Membrane potential sample traces in mSOD1^{WT} (top) and hSOD1^{G93A} SC interneurons (middle) evoked by rectangular depolarizing current pulses (bottom; 10–120 pA, 300 ms, 0.5 Hz). **B**, Mean AP frequency plotted against injected current show that the intrinsic excitability in hSOD1^{G93A} SC interneurons is significantly increased compared with mSOD1^{WT}. Statistical significance is indicated.

Table 2. Superior colliculus interneuron properties

	mSOD1 ^{WT}	hSOD1 ^{G93A}
Cell properties		
Resting membrane potential (mV)	−61 ± 3	−63 ± 2
Input resistance (MΩ)	1061 ± 171	863 ± 145
Action potential properties		
Threshold (mV above resting MP)	26 ± 3	25 ± 3
Amplitude (mV above threshold MP)	61 ± 8	84 ± 6*
Maximum rate of AP rise (mV/ms)	109 ± 24	171 ± 26
Duration (ms)	4.2 ± 0.5	3.1 ± 0.2
Half-width duration (ms)	1.8 ± 0.2	1.5 ± 0.1
Afterhyperpolarization amplitude (mV below threshold MP)	−21 ± 2	−21 ± 2
Number of cells	8	7

Averaged cell properties and AP properties (analyzed from single AP) are shown for mSOD1^{WT} and hSOD1^{G93A} SCs (P10–P12). AP threshold is relative to resting membrane for each SC recorded; AP and afterhyperpolarization amplitude are relative to AP threshold potential for each SC recorded. Note that only the AP amplitude is significantly increased in hSOD1^{G93A} SCs. Statistical significance (Student's unpaired *t* test) is indicated. Data are mean ± SEM.

amplitude in hSOD1^{G93A} SC interneurons, no differences in other AP characteristics or cell properties were found between mSOD1^{WT} and hSOD1^{G93A} SC interneurons, including maximum rate of AP rise (Table 2). Together with reports of interneuronal loss in spinal cord and cortex of human ALS patients (Maekawa et al., 2004; Stephens et al., 2006) and in transgenic

mice overexpressing mutant hSOD1 (Morrison et al., 1998), this suggests that early hyperexcitability in interneurons may also contribute to interneuronal loss at later stages in ALS.

Increased synaptic transmission in presymptomatic hSOD1^{G93A} motoneurons and interneurons

On the basis of our finding that intrinsic excitability is increased in both motoneurons and interneurons, we predicted that hyperexcitable neuronal networks in early postnatal hSOD1^{G93A} mice would generate increases in activity-dependent release of excitatory and inhibitory neurotransmitters. Enhanced activity-dependent neurotransmitter release can be measured in postsynaptic neurons as an increase in spontaneous EPSCs and IPSCs (Bellingham and Berger, 1996; O'Brien and Berger, 1999). In SC interneurons, synaptic inputs are from other local excitatory or inhibitory SC interneurons (Aamodt et al., 2000; Shi et al., 2000; Townsend et al., 2003), whereas synaptic inputs to HMs are largely from excitatory and inhibitory premotoneurons in the reticular formation lateral to the hypoglossal motor nucleus (Dobbins and Feldman, 1995; Bellingham and Berger, 1996; O'Brien and Berger, 1999).

As predicted, the mean interevent interval of sAMPAs (mSOD1^{WT} = 5.57 ± 0.88 s, *n* = 17; hSOD1^{G93A} = 2.38 ± 0.52 s, *n* = 12; *p* = 0.0067) and sGABAs (mSOD1^{WT} = 2.50 ± 0.45 s, *n* = 5; hSOD1^{G93A} = 1.07 ± 0.21 s, *n* = 11; *p* = 0.036) was significantly shorter in P10–P12 hSOD1^{G93A} SC interneurons compared with mSOD1^{WT} SC interneurons (Fig. 4A, traces; Fig. 4C for distribution of means). Mean amplitude of sAMPA (mSOD1^{WT} = 13.4 ± 0.91 pA; hSOD1^{G93A} = 15.6 ± 1.55 pA; *p* = 0.21) or sGABA (mSOD1^{WT} = 36.6 ± 3.78 pA; hSOD1^{G93A} = 33.6 ± 1.49 pA; *p* = 0.39) currents was not significantly different in SC interneurons from hSOD1^{G93A} mice (Fig. 4B for distribution of means). The change in interevent interval was attributable to increased activity-dependent transmission, as recordings of miniature quantal AMPAR currents (mAMPAs) in the presence of TTX (500 nM) demonstrated that the mean amplitude (mSOD1^{WT} = 14.3 ± 1.73 pA, *n* = 6; hSOD1^{G93A} = 14.4 ± 1.15 pA, *n* = 7; *p* = 0.92) and interevent interval (mSOD1^{WT} = 2.96 ± 1.38 s; hSOD1^{G93A} = 2.37 ± 0.67 s; *p* = 0.70) of mAMPA events in hSOD1^{G93A} SC interneurons were similar to those in mSOD1^{WT} SC interneurons (Fig. 4A, traces; Fig. 4B, C for distributions of means). Because both spontaneous EPSC activity and GABAergic IPSC activity normally increase with age in SC interneurons (Shi et al., 1997; Aamodt et al., 2000), these findings also suggested that the enhanced spontaneous transmission in SC interneuron networks was attributable to an acceleration of normal synaptic development because of increased presynaptic excitability driven by neuronal hyperexcitability.

To further investigate whether accelerated synaptic development occurred in hSOD1^{G93A} mice, we also recorded sNMDAs (Fig. 4A for traces), because the activity-dependent development of NMDA mediated responses has been well characterized for SC interneurons (Shi et al., 1997, 2000; Colonnese et al., 2003; Townsend et al., 2003, 2004; Lu and Constantine-Paton, 2004). We found that sNMDA current amplitude (mSOD1^{WT} = 9.59 ± 0.30 pA, *n* = 6; hSOD1^{G93A} = 10.13 ± 0.51 pA, *n* = 5; *p* = 0.37) or interevent interval (mSOD1^{WT} = 6.61 ± 3.13 s; hSOD1^{G93A} = 2.24 ± 0.20 s; *p* = 0.24) were not altered in hSOD1^{G93A} SC interneurons (Fig. 4A for traces; Fig. 4B, C for distributions of means), suggesting that hSOD1^{G93A} SC interneurons may have fewer synapses containing NMDA receptors, consistent with previous reports that the contributions of NMDA receptors to spon-

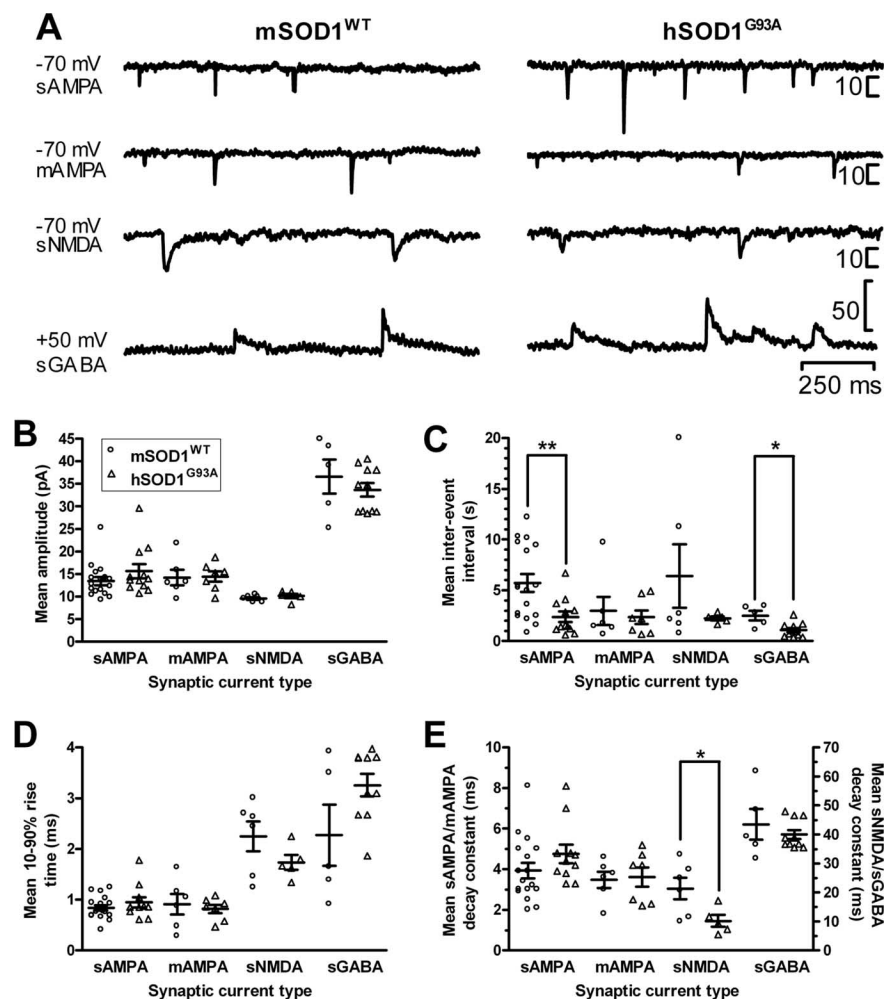


Figure 4. The frequency of spontaneous excitatory and inhibitory synaptic transmission is enhanced in SC interneurons from presymptomatic *hSOD1*^{G93A} mice. **A**, Representative spontaneous (sAMPA, sGABA, and sNMDA) and quantal (mAMPA) synaptic currents traces recorded from SC interneurons of *mSOD1*^{WT} (left) and *hSOD1*^{G93A} (right) mice. Amplitude calibration bars are 10 pA for sAMPA, mAMPA, and sNMDA traces and 50 pA for sGABA traces. Mean amplitude (**B**), interevent interval (**C**), rise time (**D**), and decay time (**E**) for the populations of sAMPA, sGABA, mAMPA, and sNMDA events recorded from each SC interneuron from *mSOD1*^{WT} (open circles) and *hSOD1*^{G93A} (open triangles) mice are shown, together with the overall mean and SEM of these values for each type of current and animal genotype superimposed over the individual cell values. Note that the frequency of sAMPA ($p < 0.01$) and sGABA ($p < 0.05$) currents are significantly increased (i.e., interevent interval is decreased) in *hSOD1*^{G93A} mice, whereas amplitude, rise time, and decay time of these current types are not significantly different. There are no significant differences in any parameters for mAMPA currents, whereas sNMDA currents showed only a significant decrease in decay time ($p < 0.05$). Student's unpaired *t* test was used to compare overall means of each parameter for *mSOD1*^{WT} and *hSOD1*^{G93A} SC interneurons.

taneous EPSCs decrease with age in SC interneurons (Shi et al., 1997). Analyses of sNMDA current kinetics also showed that the 10–90% rise time (*mSOD1*^{WT} = 2.25 ± 0.29 ms; *hSOD1*^{G93A} = 1.74 ± 0.15 ms; $p = 0.18$) was not altered, but that decay time (*mSOD1*^{WT} = 21.33 ± 3.73 ms; *hSOD1*^{G93A} = 10.2 ± 2.03 ms; $p = 0.036$) of sNMDA currents was significantly faster in *hSOD1*^{G93A} SC interneurons (Fig. 4C,D for distributions of means). Shortening of the decay-time kinetics of NMDA receptor mediated currents during development of P10–P14 SC interneurons is well characterized and can be induced by changes in the subunit composition, in which slow-decaying NR2B-containing receptors are replaced by fast-decaying NR2A-containing receptors (Shi et al., 2000; Townsend et al., 2003; Lu and Constantine-Paton, 2004). To test whether sNMDA currents are no longer predominantly mediated by NR2B-containing NMDA receptors in P10–P11 *hSOD1*^{G93A} SC interneurons, we used ifenprodil,

which preferentially antagonizes NR2B-containing NMDA receptors (Williams, 2001). As predicted, SC interneurons from P10–P11 *hSOD1*^{G93A} mice were insensitive to 5 μ M ifenprodil (control/ifenprodil = $101 \pm 2\%$, $n = 3$) suggesting that a developmental NR2B-to-NR2A subunit switch had begun earlier in *hSOD1*^{G93A} SC interneurons.

We then recorded spontaneous and/or quantal synaptic currents mediated by AMPA, NMDA, and inhibitory GABA_A and glycine receptors (sIPSCs) in early postnatal *mSOD1*^{WT} and *hSOD1*^{G93A} HMs. As for SC interneurons, we found that the mean interevent intervals of sAMPA (*mSOD1*^{WT} = 1.2 ± 0.2 s, $n = 11$; *hSOD1*^{G93A} = 0.56 ± 0.05 s, $n = 5$; $p = 0.009$) and sIPSC (*mSOD1*^{WT} = 2.53 ± 0.25 s, $n = 2$; *hSOD1*^{G93A} = 1.03 ± 0.27 s, $n = 5$; $p = 0.026$) currents were significantly decreased (Fig. 5A, traces; Fig. 5C for distribution of means), whereas mean amplitudes of sAMPA (*mSOD1*^{WT} = 12.3 ± 1.0 pA; *hSOD1*^{G93A} = 17.4 ± 3.3 pA; $p = 0.21$) and sIPSC (*mSOD1*^{WT} = 14.1 ± 6.5 pA; *hSOD1*^{G93A} = 25.1 ± 6.1 pA; $p = 0.35$) currents were not significantly different (Fig. 5A, traces; Fig. 5B for distribution of means). Similar to SC interneurons, changes in synaptic event frequency were attributable to increased activity-dependent release, because HM mAMPA mean amplitude (*mSOD1*^{WT} = 16.5 ± 1.9 pA, $n = 5$; *hSOD1*^{G93A} = 16.6 ± 2.4 pA, $n = 7$; $p = 0.97$) and interevent interval (*mSOD1*^{WT} = 2.38 ± 0.46 s; *hSOD1*^{G93A} = 1.96 ± 0.55 s; $p = 0.60$) were unchanged (Fig. 5B,C) in P4–P10 *hSOD1*^{G93A} HMs compared with *mSOD1*^{WT}. Also, as in SC interneurons, the mean amplitude (*mSOD1*^{WT} = 16.0 ± 2.1 pA, $n = 3$; *hSOD1*^{G93A} = 15.6 ± 2.4 pA, $n = 5$; $p = 0.92$), interevent interval (*mSOD1*^{WT} = 7.6 ± 2.4 s; *hSOD1*^{G93A} = 29.15 ± 14.0 s; $p = 0.29$), and rise time (*mSOD1*^{WT} = 6.4 ± 0.13 s; *hSOD1*^{G93A} =

7.0 ± 0.7 s; $p = 0.41$) of sNMDA currents were unchanged (Fig. 5B–D for distributions of means), whereas sNMDA events decayed faster (Fig. 5E for distributions of means) (*mSOD1*^{WT} = 80.4 ± 5.8 s; *hSOD1*^{G93A} = 40.8 ± 7.7 s; $p = 0.012$), suggesting that an accelerated developmental switch from NMDAR NR2B subunits to NR2A subunits was also present in motoneurons. Although the normal development of synaptic inputs to HMs is not well characterized, the similarity between changes in spontaneous synaptic activity in SC interneurons and HMs in *hSOD1*^{G93A} mice suggests that a similar acceleration of synaptic development is occurring in the neuromotor system.

Faster dendritic maturation in presymptomatic *hSOD1*^{G93A} HMs

As enhanced excitatory and inhibitory synaptic activity and changes in sNMDA decay kinetics in SC interneurons and HMs

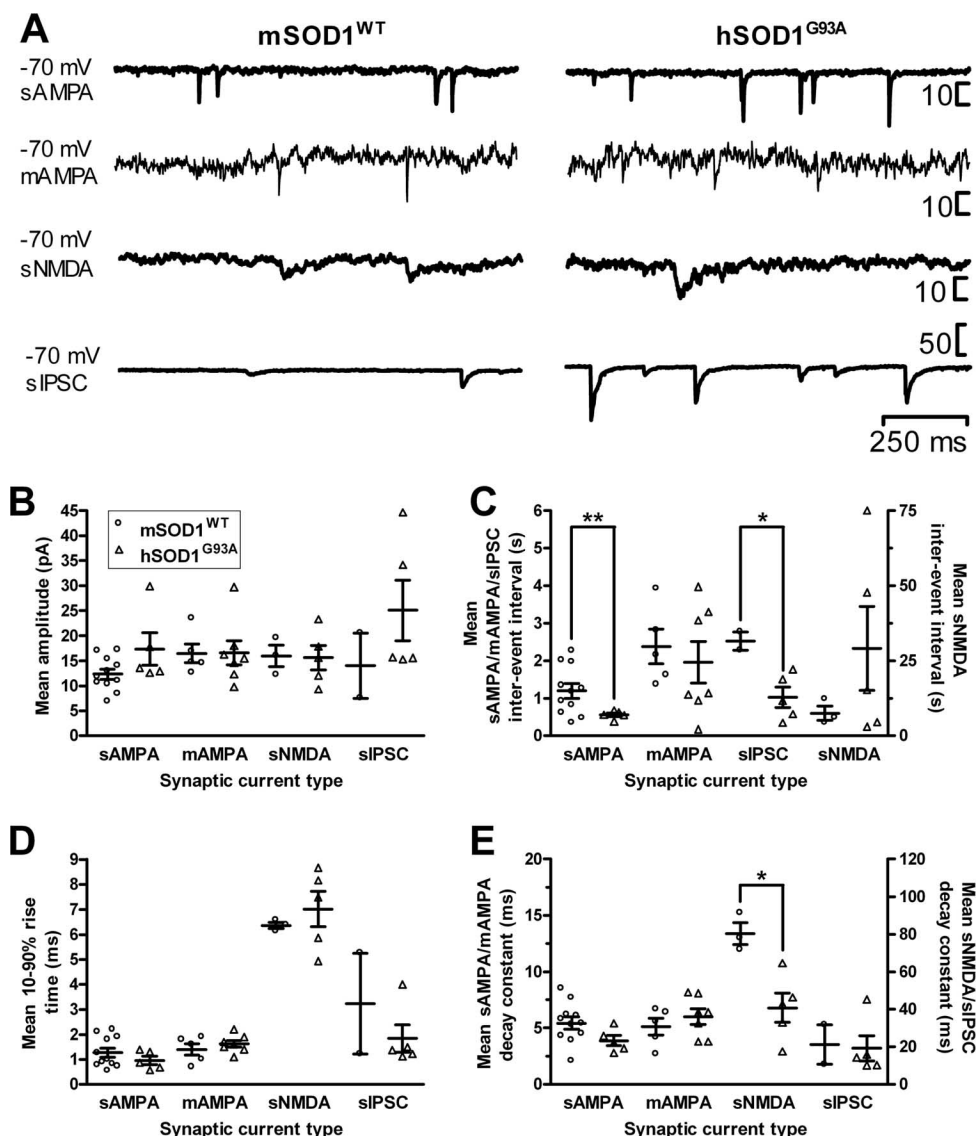


Figure 5. The frequency of spontaneous excitatory and inhibitory synaptic transmission is enhanced in HMs from presymptomatic hSOD1^{G93A} mice. *A*, Representative spontaneous (sAMPA, sIPSC, and sNMDA) and quantal (mAMPA) synaptic currents traces recorded from HMs of mSOD1^{WT} (left) and hSOD1^{G93A} (right) mice. Amplitude calibration bars are 10 pA for sAMPA, mAMPA, and sNMDA traces and 50 pA for sIPSC traces. Mean amplitude (*B*), interevent interval (*C*), rise time (*D*), and decay time (*E*) for the populations of sAMPA, sIPSC, mAMPA, and sNMDA events recorded from each HM from mSOD1^{WT} (open circles) and hSOD1^{G93A} (open triangles) mice are shown, together with the overall mean and SEM of these values for each type of current and animal genotype superimposed over the individual cell values. Note that the frequency of sAMPA ($p < 0.01$) and sIPSC ($p < 0.05$) currents are significantly increased (i.e., interevent interval is decreased) in hSOD1^{G93A} mice, whereas amplitude, rise time, and decay time of these current types are not significantly different. There are no significant differences in any parameters for mAMPA currents, whereas sNMDA currents showed only a significant decrease in decay time ($p < 0.05$). Student's unpaired t test was used to compare overall means of each parameter for mSOD1^{WT} and hSOD1^{G93A} HMs.

suggest that the hSOD1^{G93A} mutation triggers precocious maturation during early postnatal development (Aamodt et al., 2000; Shi et al., 2000; van Zundert et al., 2004), we sought to obtain additional evidence in support of this hypothesis in the neuromotor system by analyzing the morphology of HMs. To examine whether structural maturation is faster in hSOD1^{G93A} mice, we retrogradely labeled HMs by tongue injection of herpes simplex virus (HSV) carrying the green fluorescent protein (GFP) gene in P0–P1 hSOD1^{G93A} and mSOD1^{WT} littermates (Fig. 6*A–C*) (Neve et al., 2005; Olson et al., 2005). We found that structural maturation of HM dendritic architecture is detectable as withdrawal of HM dendrites crossing the brainstem midline between P6 and P9 (Fig. 6*D,E*) (cf. Núñez-Abades et al., 1994). Next we analyzed P6 brainstem sections prepared from mSOD1^{WT} and hSOD1^{G93A} mice from the same litter (Fig. 6*F,G*). As can be observed, HMs from hSOD1^{G93A} mice (Fig. 6*G*) showed significantly

fewer dendrites crossing the midline at P6 compared with control littermates (Fig. 6*F*) (mean number of dendrites in mSOD1^{WT} = 1.88 ± 0.19 , $n = 5$; in hSOD1^{G93A} = 0.17 ± 0.02 , $n = 3$; unpaired t test, $p = 0.0006$).

Altered behavioral abilities in presymptomatic hSOD1^{G93A} mice

Our observations of faster structural maturation (Fig. 6), increased intrinsic hyperexcitability (Figs. 1, 2), and altered synaptic transmission mediated by AMPA, NMDA, GABA_A, and glycine receptors (Figs. 4, 5) of SC interneurons and HMs indicate that neuronal circuitry and brain function in hSOD1^{G93A} mice is perturbed at an early postnatal age. To investigate whether alterations in neuromotor brain networks also alters early sensorimotor development, we studied six different behavioral responses (Amendola et al., 2004) in hSOD1^{G93A}, hSOD1^{WT}, and

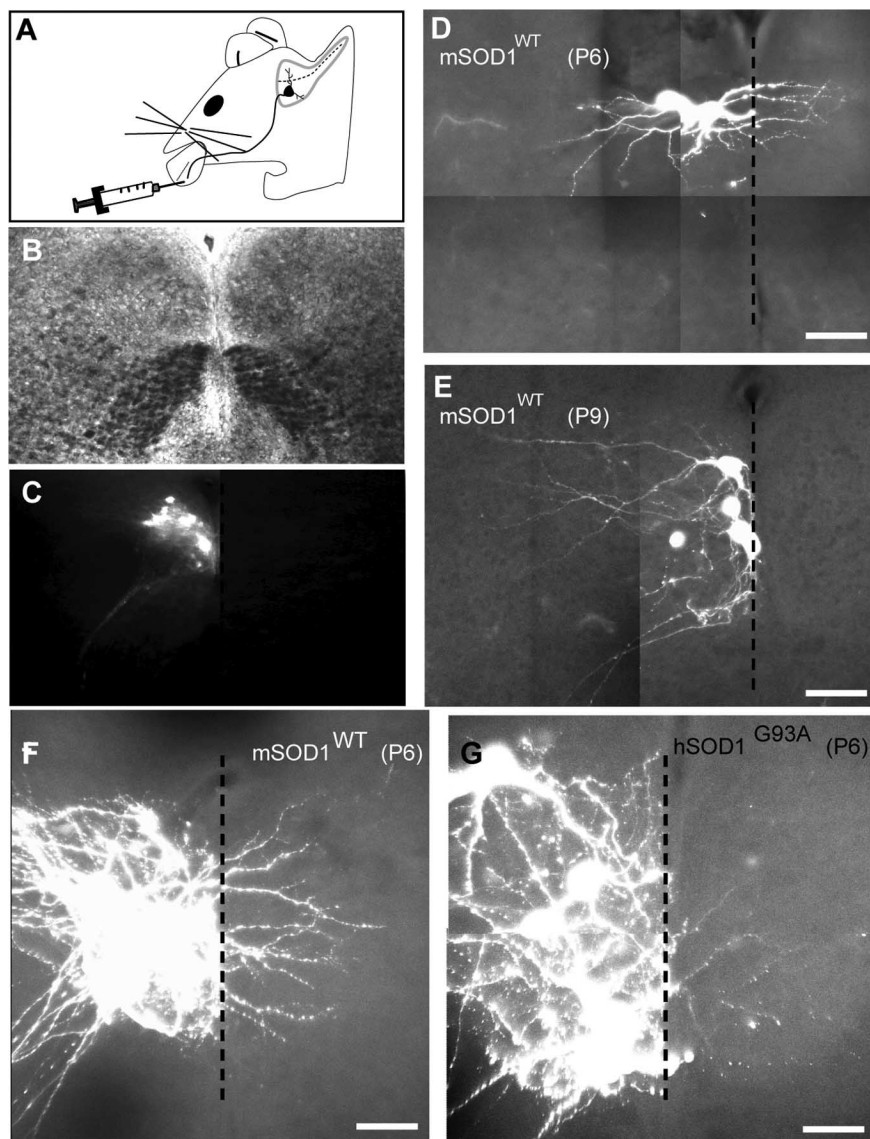


Figure 6. HMs dendrite retraction occurs earlier in presymptomatic hSOD1^{G93A} mice (P6). **A**, Schematic of HSV-GFP p1003 (2×10^8 /ml) injection in the tongue muscle at P1 to retrogradely label HMs in the ipsilateral hypoglossal nucleus (nXII). **B**, **C**, Low-magnification differential interference contrast (**B**) and fluorescent confocal (**C**) images of 350- μ m-thick 4% paraformaldehyde-fixed slices of nXII showing GFP expression in HMs. **D**, **E**, Higher-magnification images showing GFP-positive mSOD1^{WT} HMs, with labeled dendrites crossing midline (dashed line) at P6 (**D**) but not present at P9 (**E**). **F**, **G**, At P6, hSOD1^{G93A} HMs (**G**) had fewer midline-crossing dendrites than mSOD1^{WT} motoneurons (**F**). Scale bars: **D**, **E**, 100 μ m; **F**, **G**, 50 μ m.

mSOD1^{WT} mice from P1 to P12. Behavioral tests showed that the development of forelimb placing (Fig. 7*A*) was transiently reduced in P3–P4 hSOD1^{G93A} mice compared with both mSOD1^{WT} and hSOD1^{WT} mice ($p < 0.05$, χ^2 test). In contrast, neither forepaw nor hindpaw grasping (Fig. 7*C*, *E*) were significantly different between genotypes. These results suggest that development of the gross locomotor ability of the forelimb was transiently delayed in hSOD1^{G93A} animals, without alterations in the development of the fine motor control required for grasping. In addition, we also found that the righting response was transiently reduced in P2 hSOD1^{G93A} mice (Fig. 7*B*) ($p < 0.05$), suggesting that integrity of gross motor functions was transiently impaired. No differences were observed in cliff-drop aversion and vibrissae placing (Fig. 7*D*, *F*), suggesting that maturation of labyrinthine function and of vibrissae sensibility was normal in hSOD1^{G93A} mice compared with mSOD1^{WT} and hSOD1^{WT} mice, respectively.

Discussion

ALS is a CNS neurodegenerative disease in which upper and lower motoneurons are selectively targeted for death in adults. Our electrophysiological, anatomical, and behavioral data from neonatal hSOD1^{G93A} mice provide conclusive evidence that neural function is already abnormal during early development in this mouse model of FALS, occurring some 2–3 months before motoneurons degenerate and clinical symptoms appear. Moreover, we have shown that these early functional changes in neural and synaptic activity are not restricted to motoneurons, but are also present in interneurons. Together, our findings suggest a hypothesis for the etiology of FALS, in which the neonatal onset of generalized CNS hyperactivity and accelerated development may be compensated for in early life but ultimately leads to adult clinical symptoms when aging or other traumatic insults disrupt compensatory mechanisms.

Previous work has reported hyperexcitability and increased PC_{Na} in presumptive spinal motoneurons in organotypic or dissociated neuronal cultures taken from embryonic hSOD1^{G93A} mice (Kuo et al., 2004, 2005). However, long-term axotomy and the consequent loss of trophic feedback to embryonic motoneurons from muscle (Gautam et al., 1995; Li et al., 1998; Banks et al., 2005), or alterations in the neuronal environment, such as interactions with glial cells (Clement et al., 2003; Boillée et al., 2006; Di Giorgio et al., 2007; Nagai et al., 2007), are potentially a source of significant alterations in motoneuron activity and survival in these preparations. Although acute brain slice preparation causes axotomy, which can decrease synaptic contacts and change receptor expression in motoneurons (Moran and Graeber, 2004), these responses do not develop until at least 12–24 h after axotomy (González-Forero et al., 2004; Tiraihi and Rezaie, 2004), after our recordings have been made.

The correlation between increased firing rate and increased PC_{Na} in hSOD1^{G93A} motoneurons strongly suggests a causal link. This is supported by our finding that riluzole, which selectively blocks PC_{Na} (Urbani and Belluzzi, 2000), also abolishes repetitive firing in motoneurons. Our observation of significantly increased AP amplitude in HMs and SC interneurons in hSOD1^{G93A} mice suggested that Na⁺ channel density might significantly increase in hSOD1^{G93A} neurons. However, our measurements of AP maximal rate of rise, a parameter linearly coupled to total Na⁺ channel density (Kole et al., 2008), found no significant increase in either HMs or SC interneurons, ruling out increased Na⁺ channel density as a possible cause of increased PC_{Na} and AP amplitude.

As other developmental changes in motoneurons are acceler-

ated in hSOD1^{G93A} mice, one possible explanation for increased PC_{Na} without increased total Na⁺ channel density is that the normal change-over in Na⁺ channel isoforms seen in developing motoneurons occurs earlier in hSOD1^{G93A} mice. Functionally, embryonic motoneuron excitability is initially driven by Na_v1.2 and 1.3 expression, but subsequent increases in Na_v1.1 and 1.6 expression assume this role within the first 3 weeks after birth (Porter et al., 1996; Alessandri-Haber et al., 2002). The fraction of PC_{Na} produced by Na⁺ channel isoforms differs, with Na_v1.2 and 1.3 producing a small PC_{Na} (<1% of total Na⁺ current), whereas Na_v1.1 and 1.6 produces a larger PC_{Na} (>5% of total Na⁺ current) (Goldin, 1999). Thus, increased PC_{Na} could reflect the precocious appearance of Na⁺ channel isoforms with enhanced levels of persistent activity.

Other possible mechanisms for increased PC_{Na} also merit consideration. Oxidative stress can increase activity of several protein kinases (Facchinetti et al., 1998) capable of phosphorylating Na⁺ channel proteins and so changing patterns of Na⁺ channel activity. Protein kinase C (PKC) is of particular interest, because PKC activity is induced both by activity-dependent Ca²⁺ entry into neurons and by mitochondrial generation of reactive oxidation species (Facchinetti et al., 1998; Knapp and Klann, 2000; Hu et al., 2003a; Hongpaisan et al., 2004), because of direct oxidation of thiol groups on the PKC protein (Knapp and Klann, 2000). PKC activity is elevated in spinal cord tissue from hSOD1^{G93A} mice and from human ALS patients (Hu et al., 2003a,b). PKC-mediated phosphorylation of Na⁺ channels increases channel open time and decreases channel inactivation (Numann et al., 1991; Cantrell and Catterall, 2001), producing an increased PC_{Na} (Astman et al., 1998). Thus, in hSOD1^{G93A} mice, oxidative stress and Ca²⁺ entry driven by activity-dependent activation of voltage-gated Ca²⁺ channels could activate PKC, increasing PC_{Na} and motoneuron excitability. The resulting increase in Ca²⁺ influx and oxidative stress because of mitochondrial metabolic demands (Facchinetti et al., 1998) could then further activate PKC in a vicious feedback cycle. Excessive activity-dependent Ca²⁺ entry may also contribute to cell death in motoneurons, because of their limited cytosolic calcium buffering capacity, so that excess Ca²⁺ is stored in mitochondria (von Lewinski and Keller, 2005), eventually leading to structural and functional damage. Mitochondrial structure is already abnormal in motoneurons in 2- to 3-week-old hSOD1^{G93A} mice (Bendotti et al., 2001), and subsequent mitochondrial breakdown and activation of caspases (Li et al., 2000) may trigger motoneuron death.

The normal development of neuronal properties and circuitry are dependent on enhanced plasticity during a limited postnatal “critical period” (Turrigiano and Nelson, 2004). Essential elements in this plastic period include activity-dependent remodeling of receptor phenotype and neuronal morphology (van

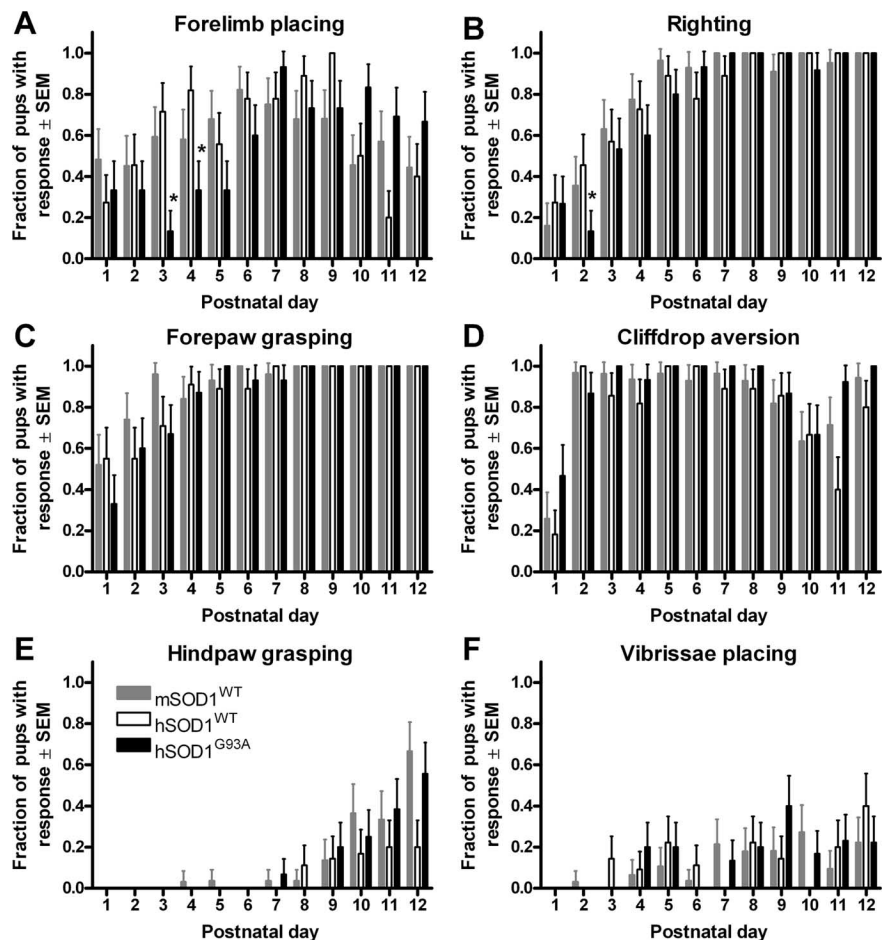


Figure 7. Transient delays in development of gross locomotor abilities in presymptomatic hSOD1^{G93A} mice are present at P2–P4. The fraction of pups displaying forelimb placing (**A**, at P3–P4 only) or righting (**B**, at P2 only) responses was lower in hSOD1^{G93A} than in mSOD1^{WT} and hSOD1^{WT} mice ($p < 0.05$, χ^2 test), whereas development of forepaw (**C**) and hindpaw (**E**) grasping, cliff-drop aversion (**D**), and vibrissae placing (**F**) were unaltered.

Zundert et al., 2004; Turrigiano and Nelson, 2004). Our data indicate that these elements are perturbed in neonatal hSOD1^{G93A} mice, consistent with our observation of enhanced neuronal activity. In both motoneurons and interneurons, we observed faster decay kinetics in NMDA glutamate receptor-mediated EPSCs, suggesting an earlier change in receptor subunit composition from NR2B-containing to NR2A containing receptors. This subunit switch has been well characterized in SC interneurons, and is normally closely dependent on retinal activity-driven synaptic inputs as the retina matures and on eye opening (Shi et al., 2000; Townsend et al., 2003; Lu and Constantine-Paton, 2004). Our data are consistent with the triggering of an earlier change in NMDA receptor composition in hSOD1^{G93A} SC interneurons, presumably because of enhanced synaptic activity even in the absence of increasing retinal inputs. Although the normal development of NMDA receptor responses is less well characterized in motoneurons, a similar change in receptor composition is also apparent. We also shown that the extensive remodeling of motoneuron dendrites occurs at least 2–3 d earlier in hSOD1^{G93A} mice. In motoneurons and other neurons, dendritic remodeling during development is regulated by consequences of neural activity, including NMDA and AMPA receptor activation (Kalb, 1994; Inglis et al., 2002), Ca²⁺ influx, and nitric oxide release (Xiong et al., 2007). All of these factors will be enhanced

by hyperactivity in hSOD1^{G93A} mice, thus accelerating the normal time course of dendrite remodeling.

Together, we show here that during very early development (P4–P12) the hSOD1^{G93A} mutation is associated with hyperexcitability (Figs. 1, 3) and increased activity-dependent excitatory and inhibitory transmission (Figs. 4, 5) in several types of central neurons. In motoneurons, hyperexcitability is associated with abnormally large PC_{Na} (Fig. 2). These changes are the earliest potentially pathogenic events yet described in the hSOD1^{G93A} mouse model of FALS, occurring before motoneuron mitochondrial dysfunction (as early as P14) and caspase-1 activation (P70), onset of limb and tongue motor weakness at 2–3 months, and end-phase disease at 4.5 months (Gurney et al., 1994; Bendotti et al., 2001; Smittkamp et al., 2008). These results are consistent with the hypothesis that increased persistent Na⁺ channel activity, causing widespread hyperexcitability and enhanced synaptic activity in the developing CNS, is a possible mechanism leading to neuronal death in hSOD1^{G93A} mice. Indirect evidence suggests that excitability of motor axons and of cortex is increased early in FALS and sporadic ALS in humans (Mogyorós et al., 1998; Vucic and Kiernan, 2006; Vucic et al., 2008). However, further work is required to determine whether widespread increases in neuronal and synaptic activity are also present in other genetic mutations associated with FALS (Pasinelli and Brown, 2006) or in sporadic ALS.

Our finding that both excitatory and inhibitory inputs to central neurons of hSOD1^{G93A} mice are more active suggests that this may reflect the attainment of a homeostatic balance in opposing synaptic activities (Turrigiano and Nelson, 2004) to actively compensate for generalized neuronal hyperexcitability. The structural changes in HM morphology (Fig. 6) and the transient disruption of some developing motor behaviors (Fig. 7) soon after birth likely reflect an abnormal period of development before the establishment of a homeostatic state in the neuromotor system. Early network changes, without the loss of neurons, may also occur in other genetically induced adult neurodegenerative diseases, such as Alzheimer and Parkinson's disease (Clarke et al., 2001; DeKosky and Marek, 2003; Palop et al., 2006). This evidence suggests a novel hypothesis for the adult onset of overt FALS symptoms, namely that they result from age-related factors (e.g., neuron loss or other traumatic insults) that cause a breakdown of homeostatic compensatory processes for neuronal hyperactivity.

It is important to note that, although our findings establish the early onset of a generalized hyperexcitability and increased synaptic activity in the neonatal hSOD1^{G93A} mouse, a mechanistic link between these phenomena and neuronal death in the adult CNS of these mice remains to be ascertained. Future experiments will determine whether the onset of motoneuron death in this animal model of FALS might be prevented or mitigated by suppression of neuronal hyperactivity in early life.

References

- Aamodt SM, Shi J, Colonnese MT, Veras W, Constantine-Paton M (2000) Chronic NMDA exposure accelerates development of GABAergic inhibition in the superior colliculus. *J Neurophysiol* 83:1580–1591.
- Alessandri-Haber N, Alcaraz G, Deleuze C, Jullien F, Manrique C, Couraud F, Crest M, Giraud P (2002) Molecular determinants of emerging excitability in rat embryonic motoneurons. *J Physiol* 541:25–39.
- Amendola J, Verrier B, Roubertoux P, Durand J (2004) Altered sensorimotor development in a transgenic mouse model of amyotrophic lateral sclerosis. *Eur J Neurosci* 20:2822–2826.
- Astman N, Gutnick MJ, Fleidervish IA (1998) Activation of protein kinase C increases neuronal excitability by regulating persistent Na⁺ current in mouse neocortical slices. *J Neurophysiol* 80:1547–1551.
- Banks GB, Kanjhan R, Wiese S, Kneussel M, Wong LM, O'Sullivan G, Sendtner M, Bellingham MC, Betz H, Noakes PG (2005) Glycinergic and GABAergic synaptic activity differentially regulate motoneuron survival and skeletal muscle innervation. *J Neurosci* 25:1249–1259.
- Bellingham MC, Berger AJ (1996) Presynaptic depression of excitatory synaptic inputs to rat hypoglossal motoneurons by muscarinic M2 receptors. *J Neurophysiol* 76:3758–3770.
- Bendotti C, Calvaresi N, Chiveri L, Prella A, Moggio M, Braga M, Silani V, De Biasi S (2001) Early vacuolization and mitochondrial damage in motor neurons of FALS mice are not associated with apoptosis or with changes in cytochrome oxidase histochemical reactivity. *J Neurol Sci* 191:25–33.
- Boillée S, Yamanaka K, Lobsiger CS, Copeland NG, Jenkins NA, Kassiotis G, Kollias G, Cleveland DW (2006) Onset and progression in inherited ALS determined by motor neurons and microglia. *Science* 312:1389–1392.
- Brown RH Jr, Robberecht W (2001) Amyotrophic lateral sclerosis: pathogenesis. *Semin Neurol* 21:131–139.
- Cantrell AR, Catterall WA (2001) Neuromodulation of Na⁺ channels: an unexpected form of cellular plasticity. *Nat Rev Neurosci* 2:397–407.
- Carlin KP, Jiang Z, Brownstone RM (2000) Characterization of calcium currents in functionally mature mouse spinal motoneurons. *Eur J Neurosci* 12:1624–1634.
- Clarke G, Lumsden CJ, McInnes RR (2001) Inherited neurodegenerative diseases: the one-hit model of neurodegeneration. *Hum Mol Genet* 10:2269–2275.
- Clement AM, Nguyen MD, Roberts EA, Garcia ML, Boillée S, Rule M, McMahon AP, Doucette W, Siwek D, Ferrante RJ, Brown RH Jr, Julien JP, Goldstein LS, Cleveland DW (2003) Wild-type nonneuronal cells extend survival of SOD1 mutant motor neurons in ALS mice. *Science* 302:113–117.
- Cleveland DW, Rothstein JD (2001) From Charcot to Lou Gehrig: deciphering selective motor neuron death in ALS. *Nat Rev Neurosci* 2:806–819.
- Colonnese MT, Shi J, Constantine-Paton M (2003) Chronic NMDA receptor blockade from birth delays the maturation of NMDA currents, but does not affect AMPA/kainate currents. *J Neurophysiol* 89:57–68.
- DeKosky ST, Marek K (2003) Looking backward to move forward: early detection of neurodegenerative disorders. *Science* 302:830–834.
- Di Giorgio FP, Carrasco MA, Siao MC, Maniatis T, Eggan K (2007) Non-cell autonomous effect of glia on motor neurons in an embryonic stem cell-based ALS model. *Nat Neurosci* 10:608–614.
- Dobbins EG, Feldman JL (1995) Differential innervation of protruder and retractor muscles of the tongue in rat. *J Comp Neurol* 357:376–394.
- Facchinetti F, Dawson VL, Dawson TM (1998) Free radicals as mediators of neuronal injury. *Cell Mol Neurobiol* 18:667–682.
- Gautam M, Noakes PG, Mudd J, Nichol M, Chu GC, Sanes JR, Merlie JP (1995) Failure of postsynaptic specialization to develop at neuromuscular junctions of rapsyn-deficient mice. *Nature* 377:232–236.
- Goldin AL (1999) Diversity of mammalian voltage-gated sodium channels. *Ann N Y Acad Sci* 868:38–50.
- González-Forero D, Portillo F, Sunico CR, Moreno-López B (2004) Nerve injury reduces responses of hypoglossal motoneurons to baseline and chemoreceptor-modulated inspiratory drive in the adult rat. *J Physiol* 557:991–1011.
- Gurney ME, Pu H, Chiu AY, Dal Canto MC, Polchow CY, Alexander DD, Caliendo J, Hentati A, Kwon YW, Deng H-X, Chen W, Zhai P, Sufit RL, Siddique T (1994) Motor neuron degeneration in mice that express a human Cu,Zn superoxide dismutase mutation. *Science* 264:1772–1775.
- Hongpaisan J, Winters CA, Andrews SB (2004) Strong calcium entry activates mitochondrial superoxide generation, upregulating kinase signaling in hippocampal neurons. *J Neurosci* 24:10878–10887.
- Hu JH, Chernoff K, Pelech S, Krieger C (2003a) Protein kinase and protein phosphatase expression in the central nervous system of G93A mSOD over-expressing mice. *J Neurochem* 85:422–431.
- Hu JH, Zhang H, Wagey R, Krieger C, Pelech SL (2003b) Protein kinase and protein phosphatase expression in amyotrophic lateral sclerosis spinal cord. *J Neurochem* 85:432–442.
- Inglis FM, Crockett R, Korada S, Abraham WC, Hollmann M, Kalb RG (2002) The AMPA receptor subunit GluR1 regulates dendritic architecture of motor neurons. *J Neurosci* 22:8042–8051.
- Ireland MF, Noakes PG, Bellingham MC (2004) P2X7-like receptor sub-

- units enhance excitatory synaptic transmission at central synapses by pre-synaptic mechanisms. *Neuroscience* 128:269–280.
- Kalb RG (1994) Regulation of motor neuron dendrite growth by NMDA receptor activation. *Development* 120:3063–3071.
- Kaminski HJ, Richmonds CR, Kusner LL, Mitumoto H (2002) Differential susceptibility of the ocular motor system to disease. *Ann N Y Acad Sci* 956:42–54.
- Knapp LT, Klann E (2000) Superoxide-induced stimulation of protein kinase C via thiol modification and modulation of zinc content. *J Biol Chem* 275:24136–24145.
- Kole MHP, Ilshner SU, Kampa BM, Williams SR, Ruben PC, Stuart GJ (2008) Action potential generation requires a high sodium channel density in the axon initial segment. *Nat Neurosci* 11:178–186.
- Kuo JJ, Schonewille M, Siddique T, Schults ANA, Fu RG, Bär PR, Anelli R, Heckman CJ, Kroese ABA (2004) Hyperexcitability of cultured spinal motoneurons from presymptomatic ALS mice. *J Neurophysiol* 91:571–575.
- Kuo JJ, Siddique T, Fu R, Heckman CJ (2005) Increased persistent Na⁺ current and its effect on excitability in motoneurons cultured from mutant SOD1 mice. *J Physiol* 563:843–854.
- Li L, Houenou LJ, Wu W, Lei M, Prevette DM, Oppenheim RW (1998) Characterization of spinal motoneuron degeneration following different types of peripheral nerve injury in neonatal and adult mice. *J Comp Neurol* 396:158–168.
- Li M, Ona VO, Guégan C, Chen M, Jackson-Lewis V, Andrews LJ, Olszewski AJ, Stieg PE, Lee J-P, Przedborski S, Friedlander RM (2000) Functional role of caspase-1 and caspase-3 in an ALS transgenic mouse model. *Science* 288:335–339.
- Lu W, Constantine-Paton M (2004) Eye opening rapidly induces synaptic potentiation and refinement. *Neuron* 43:237–249.
- Maekawa S, Al-Sarraj S, Kibble M, Landau S, Parnavelas J, Cotter D, Everall I, Leigh PN (2004) Cortical selective vulnerability in motor neuron disease: a morphometric study. *Brain* 127:1237–1251.
- Mogyoros I, Kiernan MC, Burke D, Bostock H (1998) Strength-duration properties of sensory and motor axons in amyotrophic lateral sclerosis. *Brain* 121:851–859.
- Moran LB, Graeber MB (2004) The facial nerve axotomy model. *Brain Res Rev* 44:154–178.
- Morrison BM, Janssen WG, Gordon JW, Morrison JH (1998) Time course of neuropathology in the spinal cord of G86R superoxide dismutase transgenic mice. *J Comp Neurol* 391:64–77.
- Mulder DW (1982) Clinical limits of amyotrophic lateral sclerosis. *Adv Neurol* 36:15–22.
- Nagai M, Re DB, Nagata T, Chalazonitis A, Jessell TM, Wichterle H, Przedborski S (2007) Astrocytes expressing ALS-linked mutated SOD1 release factors selectively toxic to motor neurons. *Nat Neurosci* 10:615–622.
- Neve RL, Neve KA, Nestler EJ, Carlezon WA Jr (2005) Use of herpes virus amplicon vectors to study brain disorders. *BioTechniques* 39:381–391.
- Numann R, Catterall WA, Scheuer T (1991) Functional modulation of brain sodium channels by protein kinase C phosphorylation. *Science* 254:115–118.
- Núñez-Abades PA, He F, Barrionuevo G, Cameron WE (1994) Morphology of developing rat genioglossal motoneurons studied in vitro: changes in length, branching pattern, and spatial distribution of dendrites. *J Comp Neurol* 339:401–420.
- O'Brien JA, Berger AJ (1999) Cotransmission of GABA and glycine to brain stem motoneurons. *J Neurophysiol* 82:1638–1641.
- Olson VG, Zabetian CP, Bolanos CA, Edwards S, Barrot M, Eisch AJ, Hughes T, Self DW, Neve RL, Nestler EJ (2005) Regulation of drug reward by cAMP response element-binding protein: evidence for two functionally distinct subregions of the ventral tegmental area. *J Neurosci* 25:5553–5562.
- Palop JJ, Chin J, Mucke L (2006) A network dysfunction perspective on neurodegenerative diseases. *Nature* 443:768–773.
- Pasinelli P, Brown RH (2006) Molecular biology of amyotrophic lateral sclerosis: insights from genetics. *Nat Rev Neurosci* 7:710–723.
- Porter JD, Goldstein LA, Kasarskis EJ, Brueckner JK, Spear BT (1996) The neuronal voltage-gated sodium channel, Scn8a, is essential for postnatal maturation of spinal, but not oculomotor, motor units. *Exp Neurol* 139:328–334.
- Powers RK, Binder MD (2003) Persistent sodium and calcium currents in rat hypoglossal motoneurons. *J Neurophysiol* 89:615–624.
- Raman IM, Bean BP (1999) Ionic currents underlying spontaneous action potentials in isolated cerebellar Purkinje neurons. *J Neurosci* 19:1663–1674.
- Rosen DR, Siddique T, Patterson D, Figlewicz DA, Sapp P, Hentati A, Donaldson D, Goto J, O'Regan JP, Deng HX, Rahmani Z, Krizus A, McKenna-Yasek D, Cayabyab A, Gaston SM, Berger R, Tanzi RE, Halperin JJ, Herzfeldt B, Van den Bergh R, et al. (1993) Mutations in Cu/Zn superoxide dismutase gene are associated with familial amyotrophic lateral sclerosis. *Nature* 362:59–62.
- Shi J, Aamodt SM, Constantine-Paton M (1997) Temporal correlations between functional and molecular changes in NMDA receptors and GABA neurotransmission in the superior colliculus. *J Neurosci* 17:6264–6276.
- Shi J, Townsend M, Constantine-Paton M (2000) Activity-dependent induction of tonic calcineurin activity mediates a rapid developmental downregulation of NMDA receptor currents. *Neuron* 28:103–114.
- Smittkamp SE, Brown JW, Stanford JA (2008) Time-course and characterization of orolingual motor deficits in B6SJL-Tg(SOD1-G93A)1Gur/J mice. *Neuroscience* 151:613–621.
- Stephens B, Guiloff RJ, Navarrete R, Newman P, Nikhar N, Lewis P (2006) Widespread loss of neuronal populations in the spinal ventral horn in sporadic motor neuron disease. A morphometric study. *J Neurol Sci* 244:41–58.
- Tiraihi T, Rezaie MJ (2004) Synaptic lesions and synaptophysin distribution change in spinal motoneurons at early stages following sciatic nerve transection in neonatal rats. *Brain Res Dev Brain Res* 148:97–103.
- Townsend M, Yoshii A, Mishina M, Constantine-Paton M (2003) Developmental loss of miniature N-methyl-D-aspartate receptor currents in NR2A knockout mice. *Proc Natl Acad Sci U S A* 100:1340–1345.
- Townsend M, Liu Y, Constantine-Paton M (2004) Retina-driven dephosphorylation of the NR2A subunit correlates with faster NMDA receptor kinetics at developing retinocollicular synapses. *J Neurosci* 24:11098–11107.
- Turrigiano GG, Nelson SB (2004) Homeostatic plasticity in the developing nervous system. *Nat Rev Neurosci* 5:97–107.
- Urbani A, Belluzzi O (2000) Riluzole inhibits the persistent sodium current in mammalian CNS neurons. *Eur J Neurosci* 12:3567–3574.
- van Zundert B, Yoshii A, Constantine-Paton M (2004) Receptor compartmentalization and trafficking at glutamate synapses: a developmental proposal. *Trends Neurosci* 27:428–437.
- von Lewinski F, Keller BU (2005) Ca²⁺, mitochondria and selective motoneuron vulnerability: implications for ALS. *Trends Neurosci* 28:494–500.
- Vucic S, Kiernan MC (2006) Novel threshold tracking techniques suggest that cortical hyperexcitability is an early feature of motor neuron disease. *Brain* 129:2436–2446.
- Vucic S, Nicholson GA, Kiernan MC (2008) Cortical hyperexcitability may precede the onset of familial amyotrophic lateral sclerosis. *Brain* 131:1540–1550.
- Williams K (2001) Ifenprodil, a novel NMDA receptor antagonist: site and mechanism of action. *Curr Drug Targets* 2:285–298.
- Xiong G, Mojsilovic-Petrovic J, Pérez CA, Kalb RG (2007) Embryonic motor neuron dendrite growth is stunted by inhibition of nitric oxide-dependent activation of soluble guanylyl cyclase and protein kinase G. *Eur J Neurosci* 25:1987–1997.